Cylindrical Self-Assembly and Flow Alignment of Comb-Shaped Supramolecules of Electrically Conducting Polyaniline

Mari Tiitu,[†] Nicole Volk,[†] Mika Torkkeli,[‡] Ritva Serimaa,[‡] Gerrit ten Brinke,*[,§] and Olli Ikkala*[,†]

Department of Engineering Physics and Mathematics, and Center for New Materials, Helsinki University of Technology, P.O. Box 2200, FIN-02015 HUT, Espoo, Finland, Laboratory of Polymer Chemistry, Materials Science Centre, University of Groningen, Nijenborgh 4, 9747 AG Groningen, The Netherlands, and Department of Physical Sciences, University of Helsinki, P.O. Box 64, FIN-00014, Helsinki, Finland

Received February 6, 2004; Revised Manuscript Received June 24, 2004

ABSTRACT: Electrically conducting hexagonally self-assembled nanostructures of poly(aniline) (PANI) protonated with 2-acrylamido-2-methyl-1-propanesulfonic acid (AMPSA) and hydrogen bonded with resorcinol (res), 4-ethylresorcinol (C_2res) or 4-hexylresorcinol (C_6res) are studied. Small-angle X-ray scattering (SAXS) of PANI(AMPSA)$_{0.5}$($C_n$res)$_y$ with $y = 0$, ..., 1.5 indicate cylindrical self-assembly in all cases, and the long period depends on n and y. Addition of $C_n$res leads to plasticization and an increase of conductivity of up to ca. 4 orders of magnitude until saturation is achieved upon approaching $y = 1$. Simultaneously, the temperature gradient of the conductivity $d\sigma/dT$ near the room temperature changes from positive to negative, which is reminescent to a transition from a thermally activated hopping-type to a more "metallic-like" behavior. It is suggested that, upon complexation with especially res and C_2res, the PANI chains become progressively more confined in cylinders suggesting their stretching. Overall alignment of the local self-assembled domains was also aimed. In films, anisotropic overall structure and conductivity are observed upon pressing the "melt" samples between two glass plates. In more bulky samples, so far, large amplitude oscillating shear flow leads to biaxial structural anisotropy without observable conductivity anisotropy, potentially indicating the importance of residual defects for the transport properties.

Introduction

Although a large number of conjugated polymers have been studied over the years, there exist relatively few alternatives for practical applications to combine feasible thermal and chemical stability and facile processing procedures. Among such polymers, examples are poly(pyrrole), substituted poly(thiophene)s, in particular the poly(3,4-ethylenedioxythiophene)/poly(styrenesulfonic acid) complex, and the various salts of poly(aniline), notably using substituted sulfonic acids.[1,2]

In the case of poly(aniline), PANI, understanding of the transport and structural properties has recently considerably progressed,[2−14] but still the ultimate properties of films seem not to have drastically improved from the level reached by the mid 1990s.[1,15−18] By that time, it was realized that, using surfactant-like counterions, polyelectrolyte−surfactant complexes were achieved with increased solubility and self-assembly.[1,19,20] The classic example is dodecylbenzenesulfonic acid (DBSA) which renders orthorhombic crystalline structure when a nominally stoichiometric amount of DBSA is used to protonate the iminic nitrogens of PANI, i.e., PANI(DBSA)$_{0.5}$.[21] However, such a complex is poorly soluble and infusible as are most other polyaniline salts. When the amount of DBSA is doubled i.e., PANI(DBSA)$_{1.0}$, the additional DBSA is probably hydrogen bonded to the aminic nitrogens. In this case, a lamellar self-assembly is obtained,[20] the material flows at increased temperatures, and it is soluble in, e.g., toluene.[19] Another early surfactant was dinonyl naphthalene sulfonic acid.[1,22] Lamellar self-assembly has been obtained using dialkyl or dialkoxy esters of sulfoisophthalic acid, dialkyl or dialkoxy esters of sulfophthalic acid, and the dialkyl ester of sulfosuccinic acid,[9,11−13,23] and relatively high conductivity up to ca. 200 S/cm has been demonstrated when the polymer was processed from dichloroacetic acid. However, use of less aggressive solvents typically leads to conductivities which are orders of magnitude smaller. The other early particularly feasible counterion is camphor sulfonic acid (CSA) that rendered conductivities of ca. 300 S/cm upon casting from phenolic *m*-cresol.[1,17,18] This success seems to remain still unexplained in detail, although there are suggestions based on crystallized structures[18] and models that PANI, CSA, and phenols could form molecularly matching bonds.[24] The latter hypothesis launched studies to search molecularly matching amphiphiles with several hydrogen bonding sites and new solid solvents were identified, such as the resorcinols.[10,25,26] PANI(CSA)$_{0.5}$ forms cylindrical self-assembly with 4-hexylresorcinol due to the repulsive hexyl tail.[10]

Another development is that PANI complexed with 2-acrylamido-2-methyl-1-propanesulfonic acid (AMPSA) gives highly conducting fibers, up to 2000 S/cm, when it is wet spun from dichloroacetic acid.[7,8] In this case, highly purified PANI with high molecular weight was used and the chains were stretched due to the wet spinning process, which may contribute to the high conductivity.

In this work we aimed to confine PANI protonated by AMPSA within self-assembled cylinders due to complexation with hydrogen bonded alkyl resorcinol amphiphiles, which we expected to lead to their potential stretching and modification of the transport proper-

[†] Helsinki University of Technology.
[‡] University of Helsinki.
[§] University of Groningen.

10.1021/ma0497409 CCC: $27.50
Published on Web 08/19/2004

ties. On the other hand, self-assembly leads only to local order and we aimed to impose flow (see other polymer systems[27−33]) to align the self-assembled domains and potentially to even suppress the domain boundaries which also could lead to improved charge transport.

Experimental Section

Materials. Poly(aniline) (PANI, batch EB123, size in *N*-methyl pyrrolidone (NMP) comparable to polystyrene (PS) standard of M_w ca. 50000 g/mol as measured by gel permeation chromatography, described later) was supplied by Panipol Ltd. (Finland). PANI and 2-acrylamido-2-methyl-1-propanesulfonic acid (AMPSA, Aldrich, 99%) were dried in a vacuum (10^{-2} mbar) at room temperature for 16 h before use. Resorcinol (res, Fluka, 98%), 4-ethylresorcinol (C_2res, Aldrich, 98%), and 4-hexylresorcinol (C_6res, Fluka, 98%) were used without drying due to their strong sublimation tendency. Formic acid (Riedel de Haën) had a purity of at least 98%.

GPC (SEC) Analysis. The GPC analysis of PANI was done essentially after ref 34 with some exceptions. First, 2.0 mg of PANI was dissolved in 4.0 g NMP containing 0.10 wt % LiCl. The PANI concentration was 0.050 wt %. The solution was mixed for a week, after which it was particleless in optical microscopy. The solution was filtered with a 0.45 μm pore size Millipore PTFE filter before the GPC measurement. The GPC system consisted of Waters equipment and pump. Waters Styragel HR 2, HR4, and HR6 columns were used. Polystyrene standards (M_ws 629000, 28600, 1360, 1290000, 72200, 2850, 2320000, 215000, and 131000 and polydispersities 1.03, 1.03, 1.07, 1.05, 1.02, 1.06, 1.04, 1.03 and 1.03, respectively) were measured as 0.050 wt % solutions in NMP containing 0.10 wt % LiCl. The temperature was set to 30 °C, and the carrier solvent flow was set to 0.5 mL/min. Degassed NMP containing 0.10 wt % LiCl was used as the carrier solvent.

Sample Preparation. First a 0.2 wt % PANI solution in formic acid was prepared by slowly adding PANI into formic acid while stirring.The solution was stirred for 7 days and then filtered through polypropylene prefilters (Millipore) with pore sizes 30, 10, 5, 2.5, 1.2, and 0.6 μm. The amount of insoluble material was estimated by weighing the filters before and after filtration, and was ca. 1 wt % of PANI. Then 0.5 mol of AMPSA vs 1 mol of PhN repeat units of PANI was added, the solution magnetically stirred for 1 day, and formic acid evaporated, to achieve the nominally fully protonated complex PANI(AMPSA)$_{0.5}$.

It turned out to be difficult to find a common solvent to prepare the complexes between PANI(AMPSA)$_{0.5}$ and the (alkyl)resorcinols. Dichloroacetic acid was first tried, given its feasibility as a solvent to spin highly conducting fibers.[8] The solutions, however, quickly turned pink, indicating excessively rapid ester formation. As no less acidic solvents were identified, formic acid turned out to be acceptable, if the samples were made quickly: The formic acid solutions containing PANI(AMPSA)$_{0.5}$ and resorcinol, 4-ethylresorcinol, or 4-hexylresorcinol were mixed in the nominal proportions and stirred for 20 min and then quickly evaporated on a hot plate at 40 °C and dried in a vacuum (10^{-2} mbar) at 50 °C for 1 h to remove residual formic acid. The short mixing time is used in order to minimize the unwanted esterification between formic acid and resorcinols and no color change suggestive for esterification was observed. More quantitatively, the amount of the unwanted side reaction was investigated by ^{1}H NMR. After evaporation of pure C_6res from formic acid solution the free OH groups were still observed (^{1}H NMR (d-DMSO): δ = 8.91 (s, 1 H, OH), 8.99 (s, 1 H, OH)), whereas in the presence of equimolar amount of free AMPSA the ester was formed (^{1}H NMR (d-DMSO): δ = 8.29 (s, 2 H, CH)), because the esterification is catalyzed by a strong acid. Extraction of the PANI complexes with chloroform and DMSO however show less than 5% ester formation. Ideas to remove the possible minor amounts of esters were not identified, but as the expected amount is small, formic acid was regarded as an acceptable solvent. The samples were homogeneous at the resolution of optical microscopy. As NMR and FTIR cannot easily be applied for the detailed assignment of the bondings of the present complexes, strong but indirect information supporting the complex formation could be evidenced based on SAXS, WAXS, and conductivity. Subsequently, the mixtures are denoted as PANI(AMPSA)$_{0.5}$($C_n$res)$_y$ according to the nominal compositions (Figure 1). Pure C_2res and C_6res samples were similarly prepared from formic acid, as a reference.

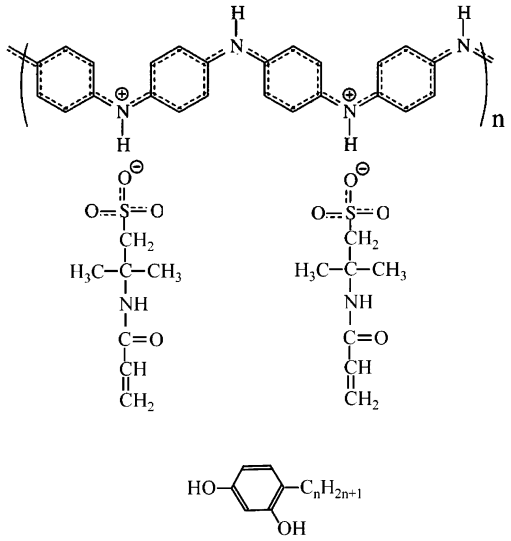

Figure 1. PANI(AMPSA)$_{0.5}$ and $C_n$res: resorcinol (n = 0), 4-ethylresorcinol (n = 2), and 4-hexylresorcinol (n = 6).

Conductivity Measurements. For conductivity measurements, a small amount of sample was placed on a glass plate, which has gold electrodes lithographically patterned on it. The sample was pressed flat between such a glass plate and microscope coverslip at ca. 125 °C, except for PANI(AMPSA)$_{0.5}$, which did not soften upon heating and was solvent-cast from formic acid instead. The dimensions of the samples were measured with Mitutoyo digimatic CD-15B slide gauge. The temperature was applied by a Linkam heating stage controlled with a Linkam TP93 controller unit. The conductivity was measured using four-point method with a Keithley 2400 SourceMeter controlled with a TestPoint program. Temperature near the sample was measured using a K-type thermocouple with Fluke 80TK thermocouple module attached to a Keithley 195A digital multimeter. A Keithley 2400 SourceMeter fed constant current into the circuit, and the voltage drop between the two inner electrodes, 1.0 mm apart from each other, was measured. The conductivity was measured for two or more cooling and heating cycles to check the reproducibility. The set heating and cooling rates were 1 °C/min, but in the actual cooling, the rate was lower since no forced cooling was used.

Large-Amplitude Oscillatory Shear Flow. Large-amplitude oscillatory shear flow was performed using Bohlin CS50 stress controlled rheometer and cone and plate geometry with a 10 mm cone diameter and the cone angle 4°. Ca. 55 mg of sample was first pressed with a Teflon mold on a hot plate at 70 °C to form a tablet. After the tablet was placed on the rheometer plate, the rheometer sample chamber was heated and kept at 70 °C for 5 min, after which the cone was brought into contact with the sample (0.150 mm gap between the lowest tip of the cone and the plate). The temperature was set at 60 °C, and the sample was kept still at least for 30 min to achieve sufficient contact. Different parameters were studied to achieve overall alignment of the samples, as based on ex-situ SAXS. The so far best parameters were as follows: frequency f = 0.5 Hz, temperature 60 °C, strain γ = 0.5, and initial stress 6000 Pa. During a typical shear flow oscillation experiment, the moduli G' and G'' decreased and the phase angle δ increased. Typical shear flow oscillation took ca. 2 h, after which the sample was quenched with liquid nitrogen to avoid relaxation of the shear aligned self-assembled structures and polymer conformations.

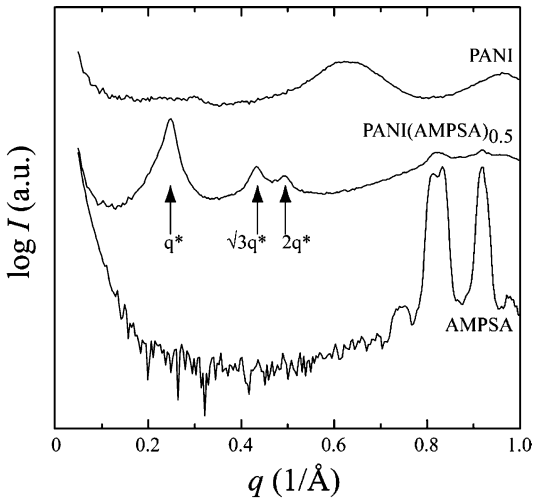

Figure 2. SAXS intensities (in a logarithmic scale) vs the magnitude of the scattering vector q for bulk samples of PANI, AMPSA and PANI(AMPSA)$_{0.5}$.

Small-Angle X-ray and Wide-Angle X-ray Scattering. Small-angle X-ray (SAXS) measurements were performed using a sealed fine-focus X-ray tube in the point-focus mode.[35] Cu Kα radiation ($\lambda = 1.54$ Å) was monochromatized with a Ni filter and a totally reflecting mirror (Huber small-angle chamber 701), and the scattered intensity was measured with a Bruker AXS Hi-Star area detector. The distance between the sample and the detector was 20 cm for SAXS and 8 cm for WAXS measurements. Magnitude of the scattering vector $q = (4\pi/\lambda) \sin \theta$, where 2θ is the scattering angle. The scattering vector was calibrated using a silver behenate standard. The intensities were corrected for absorption and nonsample scattering.

Results and Discussion

Use of formic acid as a solvent and as a medium to prepare polyaniline and other conjugated polymer complexes and blends has been described in detail.[10,32,36,37] UV−vis spectroscopy indicates that casting the emeraldine base from formic acid leads to films of protonated PANI.[37] However, formic acid is a relatively weak acid ($pK_a = 3.75$) and is quite volatile. Therefore, it is not surprising that addition of a much stronger acid, i.e., AMPSA, to an emeraldine base/formic acid solution leads to films of PANI protonated with AMPSA upon formic acid evaporation.[37]

Accordingly, in this work the nominally stoichiometric mixture of PANI and AMPSA is cast from the formic acid solvent and denoted as PANI(AMPSA)$_{0.5}$ after evaporation and drying. There is, however, a drawback to using formic acid: The conductivity of a PANI(AMPSA)$_{0.5}$ film remains rather small, i.e., on the order of 2×10^{-2} S/cm (see later Figure 5). This is in agreement with the previous results, for example PANI(CSA)$_{0.5}$ cast from formic acid renders conductivity in the range 10^{-3}−10^{-2} S/cm.[10,17]

The structure of PANI(AMPSA)$_{0.5}$ was next studied using SAXS (Figure 2) and WAXS (Figure 4). PANI cast from formic acid shows reflections that are almost identical to those reported for PANI protonated using HCl (the crystalline structure ES−I)[38] as the protonated crystalline structure is "frozen" before the formic acid can be totally removed. Different reflections are observed for PANI(AMPSA)$_{0.5}$, which is further evidence for complex formation between them. The most interesting reflections are in the SAXS-regime at $q^* = 0.249$ 1/Å, $\sqrt{3}q^*$, and $2q^*$. This suggests a hexagonally packed cylindrical structure with the Bragg distance $d = 25.2$ Å and the distance between neighboring cylinders $a = 29.1$ Å. Note that there are several fainter reflections that coincide with those of pure AMPSA and PANI. This suggests that a small amount of AMPSA actually has remained uncomplexed. However, at the resolution of optical microscopy, the samples were homogeneous and nonbirefringent. This can indicate that, if phase separated, the AMPSA crystals are of small sizes, not resolvable in optical microscopy. However, we did not regard a small amount of free AMPSA to be a major problem since, e.g., in the highly conducting fibers the optimal amount of AMPSA is even larger, i.e., nearly 0.6 mol vs PhN-repeat units, which almost certainly contains free AMPSA.[7,8]

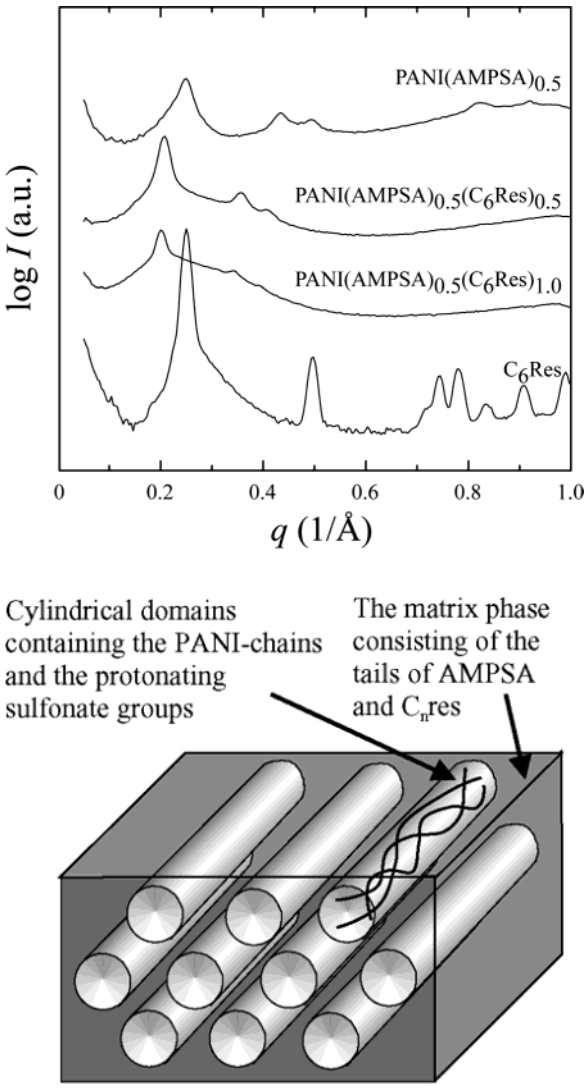

Figure 3. SAXS intensities (in a logarithmic scale) vs the magnitude of the scattering vector q for bulk samples of PANI(AMPSA)$_{0.5}$, PANI(AMPSA)$_{0.5}$(C$_6$res)$_{0.5}$, PANI(AMPSA)$_{0.5}$(C$_6$res)$_{1.0}$, and 4-hexylresorcinol (C$_6$res) and the schematics of the proposed cylindrically self-assembled structures.

Next we turn to the complexes with alkylresorcinols. All of the samples PANI(AMPSA)$_{0.5}$(C$_n$res)$_y$ with $n = 0$, 2, 6 and $y = 0.5$, and 1.0 were homogeneous at the resolution of optical microscopy and they showed no evidence of phase separation. Figure 3 depicts the SAXS reflections of PANI(AMPSA)$_{0.5}$(C$_6$res)$_{0.5}$, PANI(AMPSA)$_{0.5}$(C$_6$res)$_{1.0}$ as well as those of PANI(AMPSA)$_{0.5}$ and C$_6$res. The SAXS patterns of PANI(AMPSA)$_{0.5}$(C$_6$res)$_{0.5}$

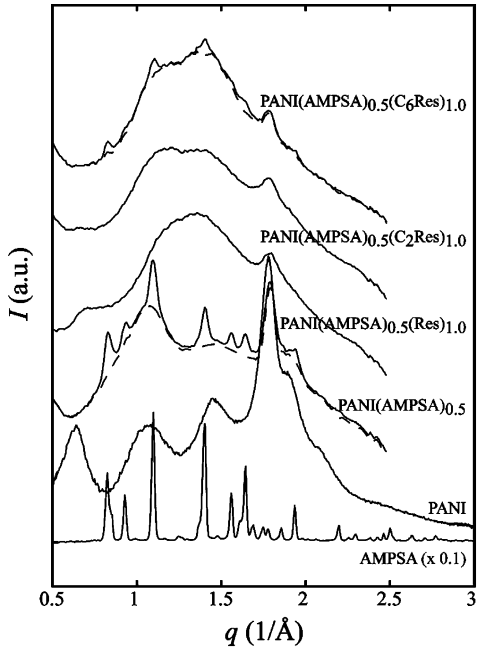

Figure 4. WAXS intensities vs the magnitude of the scattering vector q for bulk samples of PANI(AMPSA)$_{0.5}$(C$_6$res)$_{1.0}$, PANI(AMPSA)$_{0.5}$(C$_2$res)$_{1.0}$, PANI(AMPSA)$_{0.5}$(res)$_{1.0}$, PANI(AMPSA)$_{0.5}$, PANI, and AMPSA. The dashed curves represent the scattering intensity after the contribution from the crystalline AMPSA has been subtracted, which allows one to estimate the maximum amount of phase separated AMPSA.

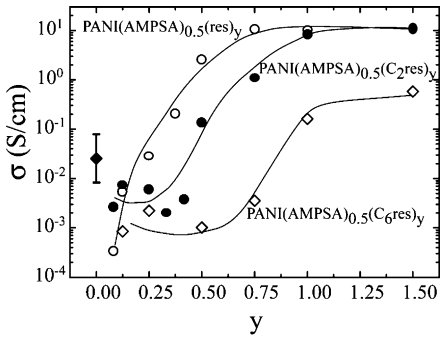

Figure 5. Room-temperature electrical conductivities for PANI(AMPSA)$_{0.5}$(C$_n$res)$_y$ vs y along the pressed films. The error bar indicates sample-to-sample variations. Within each sample, the error bar is smaller than the symbols.

Table 1. Measured Bragg Distances of the First Reflection at q^* (Å) of the Cylindrically Self-Assembled Structures of PANI(AMPSA)$_{0.5}$ and PANI(AMPSA)$_{0.5}$(C$_n$res)$_y$, Based on SAXS

	$y = 0$	$y = 0.5$	$y = 1.0$
res	25.2	25.6	25.4
C$_2$res	25.2	26.2	27.5
C$_6$res	25.2	30.3	31.1

and PANI(AMPSA)$_{0.5}$(C$_6$res)$_{1.0}$ are qualitatively different from that of C$_6$res. Like PANI(AMPSA)$_{0.5}$, these complexes show the characteristic spacing q^*, $\sqrt{3}q^*$, and $2q^*$, indicating hexagonal assembly. The Bragg distances of the first reflections at q^* are listed in Table 1. The long period increases upon adding C$_6$res. Also PANI(AMPSA)$_{0.5}$(C$_2$res)$_{0.5}$ and PANI(AMPSA)$_{0.5}$(C$_2$res)$_{1.0}$ show hexagonal self-assembly (SAXS not shown), but in this case, only a smaller increase of the long period is observed in comparison to pure PANI(AMPSA)$_{0.5}$; see Table 1. In the corresponding complexes with resorcinols, containing no repulsive alkyl tail, hexagonal assembly is observed but no essential increase in the long period was observed, see Table 1. This is an important observation and will be discussed later in some detail.

At first it seems astonishing that in some of the compositions the long periods do not increase upon adding (alkyl)resorcinols, especially using resorcinol. We will tentatively suggest that this is due to different confinement of the PANI-chains within the cylinders, which could also reflect to the observed changes in the transport properties. Note that an unambiguous explanation requires a direct assessment of the actual structures using eg. electron microscopy, which is challenging due to the required sub-20 Å resolution. As the samples containing (alkyl)resorcinols become plasticized and are able to flow upon heating, we assume that the self-assembled structures consist of hexagonally packed cylindrical domains, each containing a number of PANI chains, whereas the background is formed by AMPSA and the hydrogen bonded oligomeric C$_n$res-molecules, i.e., the plasticizing moieties. For PANI(AMPSA)$_{0.5}$ the observed Bragg distance is 25.2 Å (Figure 2, Table 1). According to the above simplistic model, one can evaluate that the diameter of the suggested PANI-core would be 21.3 Å. Using similar arguments, one can evaluate the diameters of the PANI-cores in the complexes containing (alkyl)resorcinols to be 18.4 ± 0.2, 17.6 ± 0.2, and 17.0 ± 0.1 Å for $n = 6$, 2, and 0 of PANI(AMPSA)$_{0.5}$(C$_n$res)$_{1.0}$, respectively. Therefore, adding (alkyl)resorcinols suggests confinement of the PANI-chain backbones within progressively smaller cylinders, where $n = 0$ leads to the smallest diameter. Note that this would be a significant confinement: the GPC measurements using the PS standards allow us to crudely estimate that the unconfined PANI coil size ($2R_g$) in NMP would be almost one order of magnitude larger than the suggested PANI cylinder diameter within the self-assembly of PANI(AMPSA)$_{0.5}$(C$_n$res)$_y$. A strong confinement leads to conformational changes and therefore is expected also to lead to stretching. The error bars were estimated based on SAXS and WAXS which allowed us to crudely estimate that the maximum amount of phase separated AMPSA is 13% in PANI(AMPSA)$_{0.5}$ and 5% in PANI(AMPSA)$_{0.5}$(C$_6$res)$_y$ (see also Figure 4). Also a minor part, at a maximum of 5% based on the NMR data, of C$_n$res may phase separate from PANI(AMPSA)$_{0.5}$(C$_n$res)$_y$ because of the possible esterification between (alkyl)resorcinol and formic acid, and it is also taken into account in the evaluation of the error bars.

The room-temperature electrical conductivities of PANI(AMPSA)$_{0.5}$(C$_n$res)$_y$ are shown in Figure 5 as a function of the added (alkyl)resorcinol. The samples were melt by a quick heating to 125 °C and pressed with a microscope coverslip onto glass plates which contained the measurement electrodes. The thickness of the films was 0.05−0.1 mm. The conductivity was measured along the film. An increase of conductivity is observed for larger molar fractions, i.e., $y > 0.25$, and saturation is achieved around $y = 1.0$. This is remarkable, as the conductivity increases up to 4 orders of magnitude even if the compounds are diluted upon adding the (alkyl)-resorcinols. In fact, such a behavior agrees with the above stretching hypothesis and may be regarded as an independent argument supporting it. The saturation conductivity for samples containing C$_6$res is more than one order of magnitude less than that containing C$_2$res and res. Also this observation might be explained based

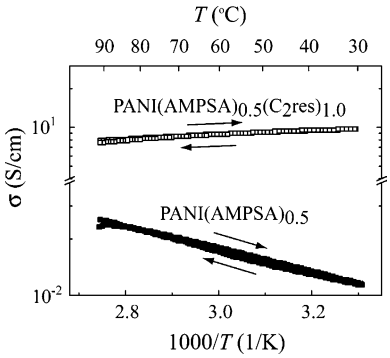

Figure 6. Electrical conductivities of PANI(AMPSA)$_{0.5}$ and PANI(AMPSA)$_{0.5}$(C$_2$res)$_{1.0}$, vs 1000/T along the pressed films. The conductivities are reversible in heating and cooling cycles.

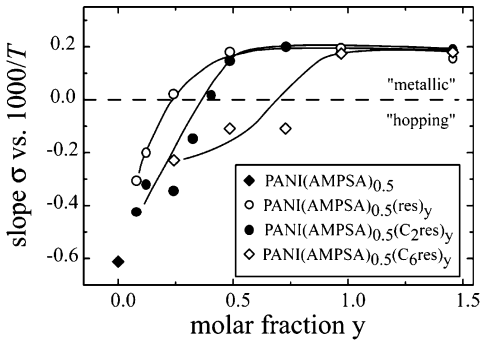

Figure 7. Slopes of conductivity plots vs 1000/T of PANI(AMPSA)$_{0.5}$ and complexes PANI(AMPSA)$_{0.5}$(C$_n$res)$_y$ vs y. Linear least-squares fitting is used to evaluate the slopes of the curves.

on the above model, as the hexyl tails are expected to increase the thickness of the insulating layers between the cylinders in comparison to cases of C$_2$res and res. Note also that addition of y much beyond the presently used values is expected to ultimately cause reduced conductivity due to excessive dilution.

Addition of (alkyl)resorcinols changes the temperature gradient of the conductivity. As an example, Figure 6 depicts the conductivities along the melt pressed films for PANI(AMPSA)$_{0.5}$ and PANI(AMPSA)$_{0.5}$(C$_2$res)$_{1.0}$ vs 1000/T near room temperature. For PANI(AMPSA)$_{0.5}$, the conductivity increases as a function of temperature which is typical for thermally activated hopping conductivity.[2,14] For PANI(AMPSA)$_{0.5}$(C$_2$res)$_{1.0}$, the conductivity decreases as a function of temperature, which may be ascribed to more "metallic-like behavior" i.e., a positive temperature coefficient of resistivity.[2,7,11,13,14] However, we emphasize that arguments related to metallic behavior far from the cryogenic temperatures have to be used with great care as a true metallic state requires finite dc-conductivity at zero temperature, positive temperature coefficient of resistivity down to zero temperature, as well as temperature-independent spin susceptibility and linear temperature dependent thermopower.[14] The positive temperature coefficient of resistivity down to the cryogenic temperatures has been observed only for few conducting polymers, really indicating metallic behavior.[14] More frequently thermally activated behavior is observed up to a finite turning point temperature, above which the "metallic-like" positive temperature coefficient of resistivity prevails.[7,11,13]

The effect of the added (alkyl)resorcinols on the temperature behavior of the conductivity along the pressed films was studied systematically and Figure 7 shows the slopes of the plots (conductivity vs 1000/T at the room temperature) vs the molar fraction on C$_n$res, i.e., y. For PANI(AMPSA)$_{0.5}$(res)$_y$ and PANI(AMPSA)$_{0.5}$(C$_2$res)$_y$, there is a transition from a thermally activated to a "metallic-like" behavior between $y = 0$ and $y = 0.5$. For PANI(AMPSA)$_{0.5}$(C$_6$res)$_y$ the transition occurs for larger values of y. We suggest that this observation may have a connection to the proposed decreased PANI core diameters upon adding (alkyl)resorcinols, where resorcinol with no tail seems to lead to the most effective confinement of the PANI-chains.

Conductivity behavior ascribed to insulator−metal transition has been previously observed for PANI protonated with CSA and plasticized with triphenyl phosphate or tritolyl phosphate.[39] These plasticized samples have a positive temperature coefficient of resistivity near room temperature, meaning their conductivities decrease when temperature increases. It was claimed that the insulator−metal transition is due to reduced disorder in the amorphous part.

Next we address the overall structure of the samples. It is well-known from other self-assembling polymers, such as block copolymers,[40] that SAXS reflections, such as in Figure 3, only indicate the existence of local domains of nanostructures and there may exist domain boundaries, lack of their common alignment, and defects between the domains. This has been visualized also for thin films of polyalkylthiophenes using STM.[41] In our case, SAXS (Figures 2 and 3) indicated hexagonal assembly for PANI(AMPSA)$_{0.5}$(C$_n$res)$_y$ without preferred alignment, which is characteristic for polydomain structures. This was anticipated, indicating the need to impose additional fields, such as flow,[27−33,42] boundary conditions due to substrates,[43] or electric field,[44,45] to align the local self-assembled structures.

First, structures of the pressed films used for the conductivity measurements (Figures 5−7) were studied in more detail. SAXS indicated that by pressing the heated and softened complexes PANI(AMPSA)$_{0.5}$(C$_n$res)$_y$ between two glass plates, the samples were macroscopically slightly aligned. This is illustrated for PANI(AMPSA)$_{0.5}$(C$_2$res)$_{1.0}$, see Figure 8. The reflections indicative for hexagonal assembly still remain as rings, which shows that there is no common single alignment of the local self-assembled structures. However, the cylinders are aligned along the substrates. Most interestingly, the anisotropy also manifests in the conductivity: the conductivity along the film is that shown in Figure 5, i.e., up to 6 S/cm, whereas perpendicular to the film surface it is several orders of magnitude less, on the order of 10^{-4} S/cm. The question exists whether the anisotropy is caused by boundary conditions due to the glass substrates or by the imposed flow due to pressing the samples between the glass plates. To answer such questions, a careful study is required where the film thickness is varied (see, e.g., ref 43) and will be postponed to a forthcoming study.

Large-amplitude oscillatory shear flow has been used to align the locally ordered self-assembled structures of block copolymers[28,30] and supramolecular polyelectrolyte systems[31,33,42] to form globally more aligned materials. It was expected that, as allowed by the plasticization, shear flow could be used to align the self-assembled domains also in the present PANI complexes. Considerable effort was used to identify proper shear flow properties; see Figure 9. Macroscopic orientation was studied ex situ with SAXS in the three perpendicular

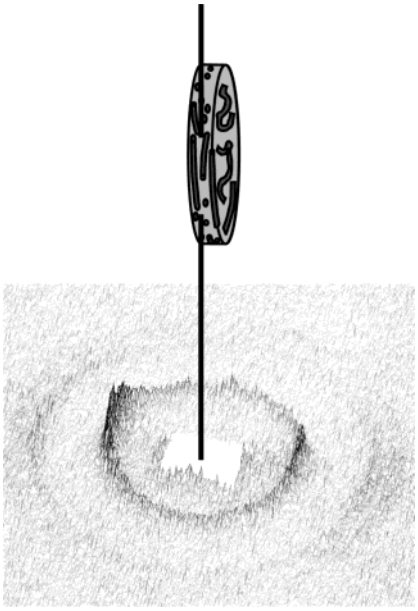

Figure 8. SAXS patterns of a pressed film of PANI(AMPSA)$_{0.5}$-(C$_2$res)$_{1.0}$. The black line indicates the incident X-ray direction. The hexagonally assembled cylinders are aligned predominantly along the glass substrates. Clear Bragg reflections show the characteristic spacing q^*, $\sqrt{3}q^*$, and $2q^*$, indicating hexagonal assembly.

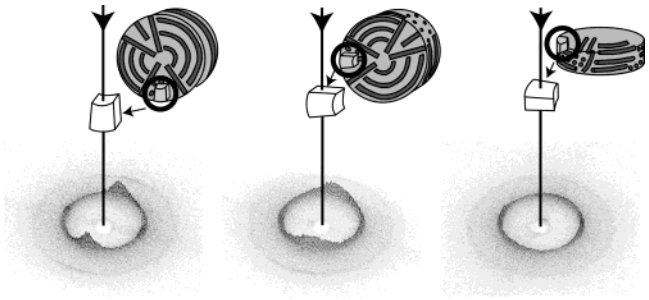

Figure 9. SAXS patterns in the radial, tangential and normal directions of PANI(AMPSA)$_{0.5}$(C$_6$res)$_{1.0}$ exposed ca. 2 h to a large amplitude oscillating shear flow at 60 °C, frequency f = 0.5 Hz, strain γ = 0.5 and initial stress 6000 Pa. Clear Bragg reflections are observed at the same q values as shown in Figure 3, with the characteristic spacing q^*, $\sqrt{3}q^*$, $2q^*$.

directions. The SAXS patterns for the so far best alignment are illustrated for PANI(AMPSA)$_{0.5}$(C$_6$res)$_{1.0}$ in Figure 9. Scattering rings characteristic for cylindrical assembly are still observed but four maxima in the radial direction indicate that there is a biaxial orientation, meaning that there are two preferred alignments of the cylindrical structures. Thus, even though the optimum conditions could not be found for well-defined single alignment, shear flow effects were demonstrated. One may wonder whether such biaxial orientation suffices to affect the conductivity. Interestingly, the measured conductivities were low, on the order of 10^{-5} S/cm, and no conductivity anisotropy is observed. The potential reason may be that the defects still dominate the transport properties.

As a conclusion on the overall order, it seems that it may be challenging to identify rheological conditions and sufficiently high shear flow to allow macroscopic overall alignment of the local cylindrically self-assembled domains of PANI. This may reflect the coiling tendency of PANI in combination with its semirigid conformation. By contrast, in totally rigid rodlike conjugated polyelectrolytes such as in polypyridine salts, even a gentle shear flow seems to efficiently align the chains, in analogy with liquid crystals.[32] It seems that in the case of PANI, surface effects may turn more straightforward to control the overall alignment of the self-assembled structures than flow field methods.

Conclusions

Polyaniline complexes were studied, as protonated by a nominally stoichiometric amount of 2-acrylamido-2-methyl-1-propanesulfonic acid and complexed with resorcinol, ethylresorcinol or hexylresorcinol, i.e., PANI-(AMPSA)$_{0.5}$(C$_n$res)$_y$ with n = 0, 2, 6 and y = 0, ..., 1.5. The structures were studied using SAXS and WAXS, and hexagonal assembly was observed for y = 0, 0.5, and 1.0. A so far tentative model was presented where the PANI−sulfonate moieties are confined in the hexagonally assembled cylindrical domains and the 2-acrylamido-2-methyl-1-propane tails and alkylresorcinols form the matrix. This model suggests that the added alkyl resorcinols confine the PANI chains to smaller cylinders, thus leading to control of conformation due to self-assembly, which in turn may indicate stretching. This model would qualitatively explain the observed SAXS patterns, plasticization of the structures, the observed increase of conductivity upon adding (alkyl)-resorcinols, and the concurrent transition from the negative to positive temperature coefficient of resistivity, which may be ascribed as a transition from thermally activated hopping transport to more metal-like behavior. A rapid pressing of "melt" complex between two glass plates rendered both conductivity and structural anisotropy. An effort was taken to achieve common alignment of the local self-assembled domains by applying shear flow. Uniaxial alignment was not achieved but the best so far rheological conditions rendered biaxial alignment. No anisotropy in conductivity was observed in that context. We expect that the present observations might pave the way toward highly conducting metallic-like complexes due to self-assembly induced structures with conformation control due to confinement.

Acknowledgment. Harri Kosonen, Riikka Mäki-Ontto, Andrew Monkman, and Panu Hiekkataipale are acknowledged for discussions and experimental help. The financial support from the Academy of Finland, Graduate School for Materials Physics, and National Technology Agency (Finland) are gratefully acknowledged. This work was carried out in the Centre of Excellence of the Finnish Academy ("Bio- and Nanopolymers Research Group", 77317).

References and Notes

(1) Cao, Y.; Smith, P.; Heeger, A. J. *Synth. Met.* **1992**, *48*, 91.
(2) Skotheim, T. A.; Elsenbaumer, R. L.; Reynolds, J. R. *Handbook of Conducting Polymers*, 2nd ed.; Marcel Dekker: New York, 1998.
(3) Reghu, M.; Yoon, C. O.; Moses, D.; Heeger, A. J.; Cao, Y. *Phys. Rev. B* **1993**, *48*, 17685.
(4) Holland, E. R.; Pomfret, S. J.; Adams, P. N.; Monkman, A. P. *J. Phys. Condens. Matt.* **1996**, *8*, 2991.
(5) Hopkins, A. R.; Rasmussen, P. G.; Basheer, R. A. *Macromolecules* **1996**, *29*, 7838.
(6) Kulszewicz-Bajer, I.; Wielgus, I.; Pron, A.; Rannou, P. *Macromolecules* **1997**, *30*, 7091.
(7) Adams, P. N.; Devasagayam, P.; Pomfret, S. J.; Abell, L.; Monkman, A. P. *J. Phys.: Condens. Matter* **1998**, *10*, 8293.
(8) Pomfret, S. J.; Adams, P. N.; Comfort, N. P.; Monkman, A. P. *Adv. Mater.* **1998**, *10*, 1351.

(9) Kulszewicz-Bajer, I.; Zagórska, M.; Niziol, J.; Pron, A.; Luzny, W. *Synth. Met.* **2000**, *114*, 125.
(10) Kosonen, H.; Ruokolainen, J.; Knaapila, M.; Torkkeli, M.; Jokela, K.; Serimaa, R.; ten Brinke, G.; Bras, W.; Monkman, A. P.; Ikkala, O. *Macromolecules* **2000**, *33*, 8671.
(11) Dufour, B.; Rannou, P.; Fedorko, P.; Djurado, D.; Travers, J. P.; Pron, A. *Chem. Mater.* **2001**, *13*, 4032.
(12) Pron, A.; Rannou, P. *Prog. Polym. Sci.* **2002**, *27*, 135.
(13) Dufour, B.; Rannou, P.; Djurado, D.; Janeczek, H.; Zagorska, M.; de Geyer, A.; Travers, J.-P.; Pron, A. *Chem. Mater.* **2003**, *15*, 1587.
(14) Kiebooms, R.; Reghu, M.; Lee, K. In *Handbook of Advanced Electronic and Photonic Materials and Devices*; Nalwa, H. S., Ed.; Academic Press: New York, 2001; Vol. 8.
(15) MacDiarmid, A. G.; Epstein, A. J. *Synth. Met.* **1994**, *65*, 103.
(16) MacDiarmid, A. G.; Epstein, A. J. *Mater. Res. Soc. Symp. Proc.* **1994**, *328*, 133.
(17) Cao, Y.; Qiu, J.; Smith, P. *Synth. Met.* **1995**, *69*, 187.
(18) Cao, Y.; Smith, P. *Synth. Met.* **1995**, *69*, 191.
(19) Cao, Y.; Smith, P.; Heeger, A. J. U.S. Patent 5,232,631, 1993.
(20) Zheng, W.-Y.; Wang, R.-H.; Levon, K.; Rong, Z. Y.; Taka, T.; Pan, W. *Makromol. Chem. Phys.* **1995**, *196*, 2443.
(21) Yang, C. Y.; Smith, P.; Heeger, A. J.; Cao, Y.; Österholm, J.-E. *Polymer* **1994**, *35*, 1142.
(22) Kinlen, P. J.; Liu, J.; Ding, Y.; Graham, C. R.; Remsen, E. E. *Macromolecules* **1998**, *31*, 1735.
(23) Olinga, T. E.; Fraysse, J.; Travers, J. P.; Dufresne, A.; Pron, A. *Macromolecules* **2000**, *33*, 2107.
(24) Ikkala, O. T.; Pietilä, L.-O.; Ahjopalo, L.; Österholm, H.; Passiniemi, P. J. *J. Chem. Phys.* **1995**, *103*, 9855.
(25) Vikki, T.; Pietilä, L.-O.; Österholm, H.; Ahjopalo, L.; Takala, A.; Toivo, A.; Levon, K.; Passiniemi, P.; Ikkala, O. *Macromolecules* **1996**, *29*, 2945.
(26) Ikkala, O.; Pietilä, L.-O.; Cao, Y.; Andreatta, A. U. S. Patent 5,783,111, 1998.
(27) Gupta, V. K.; Krishnamoorti, R.; Kornfield, J. A.; Smith, S. D. *Macromolecules* **1995**, *28*, 4464.
(28) Sänger, J.; Gronski, W.; Leist, H.; Wiesner, U. *Macromolecules* **1997**, *30*, 7621.
(29) Zhang, Y.; Wiesner, U. *J. Chem. Phys.* **1997**, *106*, 2961.
(30) Chen, Z.-R.; Kornfield, J. A.; Smith, S. D.; Grothaus, J. T.; Satkowski, M. M. *Science* **1997**, *277*, 1248.
(31) de Moel, K.; Mäki-Ontto, R.; Stamm, M.; Ikkala, O.; ten Brinke, G. *Macromolecules* **2001**, *34*, 2892.
(32) Knaapila, M.; Torkkeli, M.; Horsburgh, L. E.; Pålsson, L.-O.; Jokela, K.; Serimaa, R.; ten Brinke, G.; Monkman, A. P.; Ikkala, O. *Appl. Phys. Lett.* **2002**, *81*, 1489.
(33) Ruotsalainen, T.; Torkkeli, M.; Serimaa, R.; Mäkelä, T.; Mäki-Ontto, R.; Ruokolainen, J.; ten Brinke, G.; Ikkala, O. *Macromolecules* **2003**, *36*, 9437.
(34) Wei, Y.; Hsueh, K.; Jang, G.-W. *Macromolecules* **1994**, *27*, 518.
(35) Torkkeli, M.; Serimaa, R.; Ikkala, O.; Linder, M. *Biophys. J.* **2002**, *83*, 2240.
(36) Angelopoulos, M.; Asturias, G. E.; Ermer, S. P.; Ray, A.; Scherr, E. M.; MacDiarmid, A. G.; Akhtar, M. A.; Kiss, Z.; Epstein, A. J. *Mol. Cryst. Liq. Cryst.* **1988**, *160*, 151.
(37) Zagorska, M.; Taler, E.; Kulszewicz-Bajer, I.; Pron, A.; Niziol, J. *J. Appl. Polym. Sci.* **1999**, *73*, 1423.
(38) Pouget, J. P.; Józefowicz, M. E.; Epstein, A. J.; Tang, X.; MacDiarmid, A. G. *Macromolecules* **1991**, *24*, 779.
(39) Fedorko, P.; Djurado, D.; Trznadel, M.; Dufour, B.; Rannou, P.; Travers, J. P. *Synth. Met.* **2003**, *135*−*136*, 327.
(40) Hamley, I. W. *The physics of block copolymers*; Oxford University Press: Oxford, England, 1998.
(41) Mena-Osteritz, E.; Meyer, A.; Langeveld-Voss, B. M. W.; Janssen, R. A. J.; Meijer, E. W.; Bäuerle, P. *Angew. Chem., Int. Ed.* **2000**, *39*, 2680.
(42) Mäkinen, R.; Ruokolainen, J.; Ikkala, O.; de Moel, K.; ten Brinke, G.; De Odorico, W.; Stamm, M. *Macromolecules* **2000**, *33*, 3441.
(43) Knoll, A.; Horvat, A.; Lyakhova, K. S.; Krausch, G.; Sevink, G. J. A.; Zvelindovsky, A. V.; Magerle, R. *Phys. Rev. Lett.* **2002**, *89*, 035501.
(44) Thurn-Albrecht, T.; Schotter, J.; Kästle, G. A.; Emley, N.; Shibauchi, T.; Krusin-Elbaum, L.; Guarini, K.; Black, C. T.; Tuominen, M. T.; Russell, T. P. *Science* **2000**, *290*, 2126.
(45) Böker, A.; Elbs, H.; Hänsel, H.; Knoll, A.; Ludwigs, S.; Zettl, H.; Urban, V.; Abetz, V.; Muller, A. H. E.; Krausch, G. *Phys. Rev. Lett.* **2002**, *89*, 135502.

MA0497409